Jo *et al.*
Journal of Analytical Science and Technology (2023) 14:21
https://doi.org/10.1186/s40543-023-00385-2

Journal of Analytical Science and Technology

RESEARCH ARTICLE Open Access

Sulfur reduction distillation of sulfides and verification of the effect of sulfur isotopic fractionation during pretreatment

Jaeguk Jo[1], Toshiro Yamanaka[2], Hitoshi Chiba[3] and Dongbok Shin[1*]

Abstract

Toxic gases can be emitted when sulfides form compounds with heavy metals; thus, a series of pretreatments are required prior to the analysis of sulfur isotope ratios to remove unnecessary elements. In addition, it is necessary to verify the effect of sulfur isotope fractionation caused by the plurality of sulfides comprising different sulfide species during the pretreatment process. In this study, $H_2S_{(gas)}$ was extracted from mixed sulfides comprising pyrite and galena and reacted with mixed acids (i.e., HCl + HI + H_3PO_2) at 200 °C, in sealed conditions filled with N_2. Subsequently, $CdS_{(s)}$ was precipitated from the reaction with $H_2S_{(gas)}$ in a trap filled with $Cd(CH_3COO)_{2(aq)}$. $CdS_{(s)}$ was then ionized to ${SO_4}^{2-}{}_{(aq)}$ after reacting with $H_2O_{2(l)}$, followed by the addition of $BaCl_{2(l)}$ to precipitate $BaSO_{4(s)}$. The sulfur isotope values of the products (barite: av. 5.9‰) were lower than those of the reactants (sulfides: av. 6.9‰); this is attributed to the preferential fractionation of galena with a low isotope ratio when converting sulfide to $H_2S_{(gas)}$. Therefore, in the pretreatment process for the sulfur isotope analysis of a sample composed of a sulfide mixture, the effect of isotope fractionation between sulfur species should be considered.

Keywords Sulfur reduction, Barium sulfate, Pyrite, Galena, Sulfur isotope fractionation

Introduction

Sulfur, one of the major constituents of the Earth's crust, is a dominant nonmetal element occurring in ore deposits and exists in the form of sulfates or sulfides in a wide range of sulfur isotopic compositions. Sulfur has four stable isotopes; ^{32}S, ^{33}S, ^{34}S, and ^{36}S, and their abundances in nature are 95.02%, 0.75%, 4.2%, and 0.017%, respectively (MacNamara and Thode 1950). In addition, the stable isotope ratio for a specific material is expressed as $^{34}S/^{32}S$, using two relatively abundant sulfur species, and $\delta^{34}S$ (‰) according to Eq. (1) using the standard material (CDT: Canyon Diablo Troilite) (Beaudoin et al. 1994).

$$\delta^{34}S = \frac{(^{34}S/^{32}S_{\text{sample}} - {}^{34}S/^{32}S_{\text{CDT}})}{(^{34}S/^{32}S_{\text{CDT}})} \times 1000 \quad (1)$$

Sulfur reduction distillation methods for organic and inorganic samples have been undertaken in various research (Toshiyasu et al. 1957; Ault and Kult 1959; Thode et al. 1961; Sasaki et al. 1979; Arnold et al. 2014). Toshiyasu et al. (1957) proposed a sulfur reduction distillation method that required a complicated pretreatment process, for example, after preparing a "Kiba" reagent, which is a mixture of stannous chloride ($SnCl_2$) and phosphoric acid (H_3PO_4), sulfide minerals were dissolved at high temperatures to extract hydrogen sulfide (H_2S) and passed through a carbon dioxide (CO_2) trap to expel air. Zinc acetate ($Zn(CH_3COO)_2$ was then added to precipitate zinc sulfide (ZnS), and bromine water ($HBrO_3 + H_2O$) was added to produce sulfate ions

*Correspondence:
Dongbok Shin
shin@kongju.ac.kr
[1] Department of Geoenvironmental Sciences, Kongju National University, Gongju 32588, South Korea
[2] Department of Ocean and Environmental Sciences, Tokyo University of Marine Science and Technology, Tokyo 108-8477, Japan
[3] Graduate School of Natural Science and Technology, Okayama University, Okayama 700-8530, Japan

(SO_4^{2-}). Barium hydroxide ($Ba(OH)_2$) was added again to precipitate barium sulfate ($BaSO_4$). In the pretreatment process, the zinc sulfide precipitate adhered to the wall of the glass tube and was back-titrated using iodine solution (I_2) with sodium thiosulfate ($Na_2S_2O_3$) solution (Toshiyasu et al. 1957).

Sasaki et al. (1979) improved the sulfur reduction distillation method that uses the "Kiba" reagent by allowing nitrogen gas (N_2) to flow through a distillation line to minimize its contact with oxygen. The sulfur extracted from the reactants was precipitated as zinc sulfide, and glacial acetic acid (CH_3COOH) and silver nitrate ($AgNO_3$) were added to precipitate silver sulfide (AgS), which was then recovered using a quartz wool filter. However, when using the "Kiba" reagent, the sulfur extraction efficiency is poor for chalcopyrite ($CuFeS_2$), arsenopyrite (FeAsS), and molybdenite (MoS_2) (Sasaki et al. 1979).

Thode et al. (1961) devised a sulfur reduction distillation method using the "Thode" reagent by mixing iodic acid (HI), hydrochloric acid (HCl), and hypophosphorous acid (H_3PO_2). In this method, the "Thode" reagent and sulfide sample are reacted at high temperatures under nitrogen gas flow to extract H_2S, which is then reacted with cadmium acetate ($Cd(CH_3COO)_2$), which is first replaced by cadmium sulfide (CdS), and $AgNO_3$ is then added to recover silver sulfide (Ag_2S). However, in this method, the excess chlorine ions (Cl^-) react with $AgNO_3$ to precipitate silver chloride ($AgCl_2$) and chlorine gas (Cl_2) generated after combustion in the mass spectrometer contaminates the gas chromatography column (GC-Column) and causes an increase in the sulfur isotope error range, owing to the memory effect.

When sulfur isotope analysis is performed on As-bearing sulfide minerals (e.g., NiAs, $NiAs_2$, and $CoAs_2$), there are risk factors to consider during the handling and storage processes of the sample. In addition, corrosive gases generated during combustion cause contamination within mass spectrometers used in isotope analyses. Accordingly, Spangenberg et al. (2022) performed sulfur isotope analysis by recovering sulfur in the form of stable $BaSO_4$ as an alternative method, and showed various crystallinities (84–98%) of barite and reproducibility of sulfur isotope values (±0.5‰).

Generally, sulfide minerals produced in metallic ore deposits exhibit limited physical separation because multiple sulfide minerals can coexist under various physicochemical conditions and occur as phenocrysts or microinclusions (Abraitis et al. 2004; Román et al. 2019; Hutchison et al. 2020; Ren et al. 2021). Consequently, when performing a series of analyses of sulfide minerals forming a sulfide composite (e.g., FeS_2, PbS, and ZnS) that undergo different sulfur isotopic fractionation depending on temperature changes, a review of the isotopic fractionation effect between sulfur species is required (Sakai 1968; Bachinski 1969; Grootenboer and Schwarcz 1969; Salomons 1971; Li and Liu 2006; Liu et al. 2015; Zhang 2021). For instance, galena tends to have a larger sulfur isotopic fractionation factor for H_2S than other sulfide minerals, in accordance with the decrease in temperature (Ohmoto and Goldhaber 1997). Against the background of the above-mentioned points, in this study, a pretreatment process was performed on a sulfide mixture comprising pyrite and galena, and the fractionation effect on the sulfur isotope ratio between the reactants and products was examined.

Materials and methods

Reagents

HI (200 ml, 57%), H_3PO_2 (100 ml, 50–52%), and HCl (330 ml, 35–37%) were placed together with a boiling stone, and a gas line was assembled. Thereafter, nitrogen gas (N_2, 99.9999%) was slowly fed through the pretreatment line to remove internal air. The system was then heated slowly and maintained for approximately 60 min from the time the mixed acid was boiled to release all the sulfur added during the reagent manufacturing process. The mixed acid prepared through this process was stored in a brown bottle to block the photooxidation reaction of iodine. Secondary purified water was used to remove the water-soluble gas generated during the pretreatment process, and cadmium acetate ($Cd(CH_3COO)_2$), hydrogen peroxide (H_2O_2), and barium chloride ($BaCl_2$) were used for sulfur extraction and concentration.

Sulfur reduction pretreatment

Because the pretreatment process must be performed in an oxygen-blocked environment, the line was assembled under anaerobic conditions (Fig. 1). Completely dried sulfide powder (<200 mesh) composed of pyrite and galena was set in a reaction flask, a distilled water trap for capturing water-soluble gas and a cadmium acetate trap for capturing sulfide gas were installed, and a mixed acid ($HCl + HI + H_3PO_2$) was injected into the reaction flask until the sulfide powder was fully sunken. Thereafter, the cooling water was circulated outside the gas flow path connected to the upper part of the reaction flask, and the heating mantle surrounding the reaction flask was heated to 200 °C. During the boiling process, the gas released from the reactants reaches the distilled water trap through the cooling water line, and in this process, water-soluble gas is captured. Among the released gases, H_2S reaches the cadmium acetate trap together with nitrogen gas, where it is precipitated as CdS according to Eq. (2):

$$H_2S_{(gas)} + Cd(CH_3COO)_{2(aq)} \rightarrow CdS_{(s)} \downarrow + 2CH_3COOH_{(aq)} \quad (2)$$

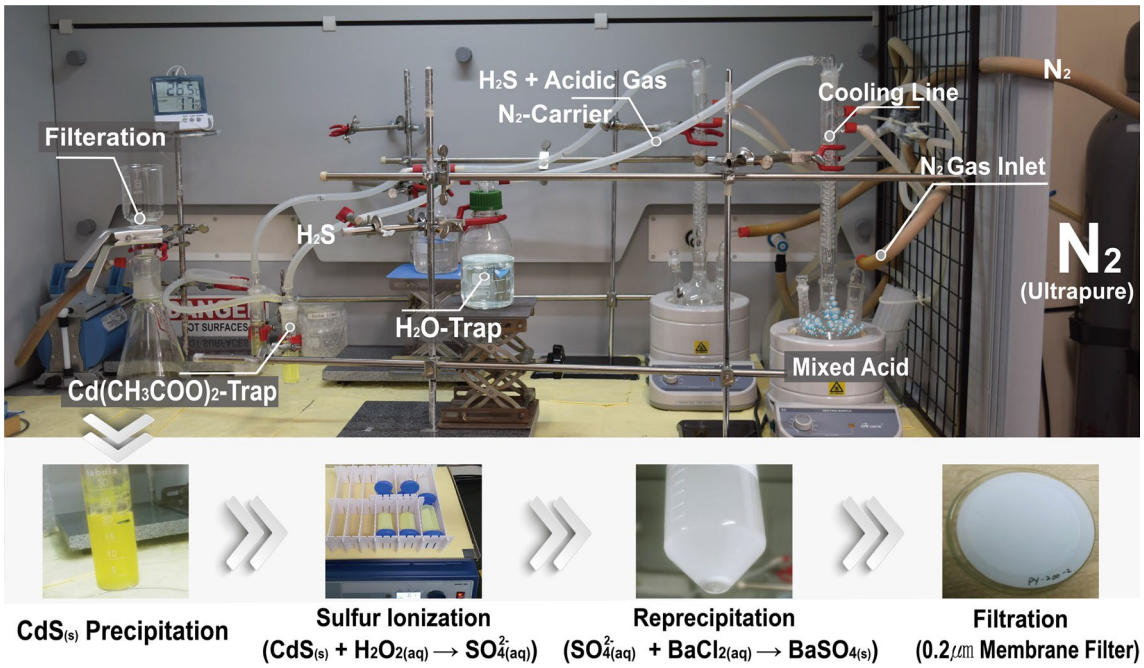

Fig. 1 Photographs displaying the sulfur reduction distillation process in this study

After boiling, it was maintained for approximately 60 min to fully react between the mixed acid and sulfide powder. The reaction flask was then cooled slowly by lowering the heating mantle temperature, and the precipitated CdS was transferred to a 50 ml centrifugal tube and ionized to sulfate (SO_4^{2-}) by injecting 30% H_2O_2 on an orbital shaker at 60 rpm for 9 h. Thereafter, 1 mol of $BaCl_2$ was injected to precipitate $BaSO_4$ according to reaction Eq. (3). $BaSO_4$ was subsequently collected using a filtration device equipped with a membrane filter (0.2 μm) and then dried in an oven at 60 °C for 9 h.

$$SO_{4(aq)}^{2-} + BaCl_2 \rightarrow BaSO_{4(s)} + 2Cl_{(aq)}^{-} \quad (3)$$

Analytical method

The sulfide minerals that were used as reactants were obtained from the Subok Pb–Zn deposit in Jecheon, South Korea. After crushing, the samples were hand-picked under a stereomicroscope. X-ray diffraction (XRD) analysis was performed using a Rigaku Mini-Flex600 instrument provided at the Center for Research Facilities in Kongju National University under the conditions of Cu-Kα (λ = 1.5418 Å), 40 kV, 15 mA, 2θ, 3–90°, 0.01 step, and 10 s. Match! ver. 3.14 Build 233 software was used to perform mineral identification and semi-quantitative phase analysis of the sulfide powder using the Rietveld refinement method.

Field emission scanning electron microscopy (FE-SEM) and Energy-dispersive X-ray spectroscopy (EDS) analyses were performed on the samples before the addition of sulfide minerals and after the precipitation of $BaSO_4$, respectively, using a JEOL (JXA-8530F PLUS) device housed at the Instrumental Analysis Center in Gyeongsang National University under an accelerating voltage of 15 kV. The samples were mounted in a cylindrical shape using epoxy and hardener, and the analysis surface was then polished sequentially down to 0.25 μm of abrasive particle size and coated with conductive carbon.

A Flash 2000 elemental analyzer (EA) installed at the Center for Research Facilities at Kongju National University was used to measure the sulfur content of the reaction product; the analysis error was better than ± 0.01 wt.%. The sulfur isotope analysis of the sulfide powder was performed using an IsoPrime EA, GV Instruments Isotope ratio mass spectrometer (IRMS) provided at Tokyo Maritime and Ocean University; the analysis error was ± 0.2‰. The sulfur isotope analysis of the reaction product, barite, was performed using an Isoprime/Delta V instrument provided at the Ochang Center of the Korea Basic Science Institute, with an analysis error of ± 0.2‰. Prior to the sulfur isotope analyses, the sample was mixed with vanadium pentoxide (a comburent) at a ratio of 1:10, sealed in an 8 × 5 mm tin capsule, and then dropped from the autosampler into a copper reaction tube. In a metallic copper tube heated to 1050 °C, the sample was pyrolyzed by flash combustion (~ 1,500 °C)

using O_2 supplied with helium gas (119 ml/min), and the unnecessary oxygen was removed and reduced to SO_2 by metallic copper. Thereafter, an oxygen isotope exchange reaction was performed with high-temperature quartz wool to maintain the oxygen isotope ratio of SO_2 at a constant. For example, because the 66/64 ratio can be affected by the oxygen isotope ratio, it must be constantly adjusted. The moisture remaining in the samples was captured using magnesium perchlorate ($Mg(ClO_4)_2$). Depending on the sample, CO_2 may be generated from impurities; however most are separated from SO_2 while passing through the GC-column. The SO_2 separated from the reaction product through the above process was guided to the ion source line together with the standard gas. In this section of the system, gas molecules are ionized and accelerated through interactions with an electron beam (electron ionization, EI), and mass separation occurs while passing through a magnetic field. The $^{34}S/^{32}S$ ratio was measured using a dual-collector mass spectrometer and was subsequently corrected by comparison with reference gases such as NBS-127 and MSS-3 (Halas and Szaran 2001; Yanagisawa and Sakai 1983).

Results and discussion

Phase change according to pretreatment process

According to the XRD analysis, the sulfide powder that was used in the pretreatment reaction consisted of pyrite (e.g., 1.63 Å, 2.70 Å, and 2.42 Å) and galena (e.g., 3.42 Å, 2.96 Å, and 2.09 Å; Fig. 2A), and based on the Rietveld refinement method, they accounted for 82% and 18% in contents, respectively. According to the backscattered electron image analysis of the sulfide sample, galena coexists with pyrite as a microinclusion of a few micrometers or a phenocryst of approximately 2 mm in pyrite (Fig. 3A and B). The recrystallized product after the pretreatment reaction was a typical orthorhombic barite composed of $BaSO_4$ (COD No. 96–900-0160: $a = 8.884$ Å, $b = 5.458$ Å, $c = 7.153$ Å, $\alpha = \beta = \gamma = 90°$; i.e., $a = 8.886$ Å, $b = 5.443$ Å, $c = 7.154$ Å; Fig. 2B), which appeared as a spherical amorphous aggregate or ellipsoid with a distinct (001) growth plane under the backscattered electron image (Fig. 3C).

The presence of single-crystal barite confirmed from the backscattered electron image, XRD analysis, and EDS analysis suggests that the sulfur in the reactants, comprising pyrite and galena, was effectively extracted and recrystallized through the sulfur reduction distillation process using a mixed acid (Figs. 2B, 3C and F). However, according to the EDS analysis, the sulfur content of barium sulfate was 12.8–13.5 wt.% (av. 13.2 wt.%, $n = 4$; Table 1), while that of the bulk barite samples measured by EA analysis yielded lower values, 10.9 wt.% in average (10.5–11.4 wt.%, $n = 11$; Table 2). It is presumed to be attributed to the technical limit of the elemental analyzer. Although vanadium pentoxide (V_2O_5) has been used to improve the combustion rate of sulfur in EA/IRMS, the complete recovery of combusted sulfur gas is still restricted (Monaghan et al. 1999; Studley et al. 2002; Spangenberg et al. 2022).

Usefulness of sulfur reduction distillation of sulfides

In metallic ore deposits formed under the influence of magmatic-hydrothermal activities, sulfide minerals can be combined with various metallic elements (e.g., Cd, Pb, Ag, W, Mo, Hg, and As); therefore, for effective sulfur isotope analysis, a series of pretreatment processes are required to remove contaminants from the analyzed elements. Sulfide minerals (e.g., FeAsS, CoAgS, and HgS) combined with mercury or arsenic require caution when treated because they emit toxic gases (Pokrovski et al. 2002; Basu and Schreiber 2013).

Spangenberg et al. (2022) pointed out the device contamination and memory effects that may occur during sulfur isotope analysis of sulfide minerals containing arsenic; for example, to analyze the sulfur isotope composition of arsenide with low sulfur content (total sulfur < 1 wt.%), a large amount of sample must be burned. In this process, excess non-analyzed gases are introduced into the ion source line (Spangenberg et al. 2022). This memory effect causes excess gas and atoms generated in the previous sample to remain in various parts of the device, including the GC-column, causing the problem of the previously accumulated gas affecting the analysis value of the next sample in the process of successive sample analysis (Grassineau 2006). In this study, impurities were separated from the reactant through a series of sulfur reduction distillation processes because they were rarely included in the high-purity form of barite (Table 1, Fig. 2B); thus, the memory effect on the sulfur isotope analysis of each sample would be negligible.

Sulfur isotope fractionation effect

In sulfide deposits associated with magmatic-hydrothermal systems, sulfur isotope values are used as an important tool that reflects the origin (e.g., magma, seawater, and organic matter) and behavior (e.g., sulfate reduction and fluid–rock interactions) of sulfur and environmental parameters related to sulfide precipitation (e.g., temperature, oxygen fugacity, and pH) (Kawasumi and Chiba 2017; Hutchison et al. 2020). Because the $^{32}S/^{34}S$ distribution between coexisting sulfide minerals occurs systematically in accordance with the sulfur-metal bond strength, the consistent sulfur isotope fractionation mechanism under equilibrium conditions provides information on the origin of elements and formation temperature of minerals, which are important for the interpretation of

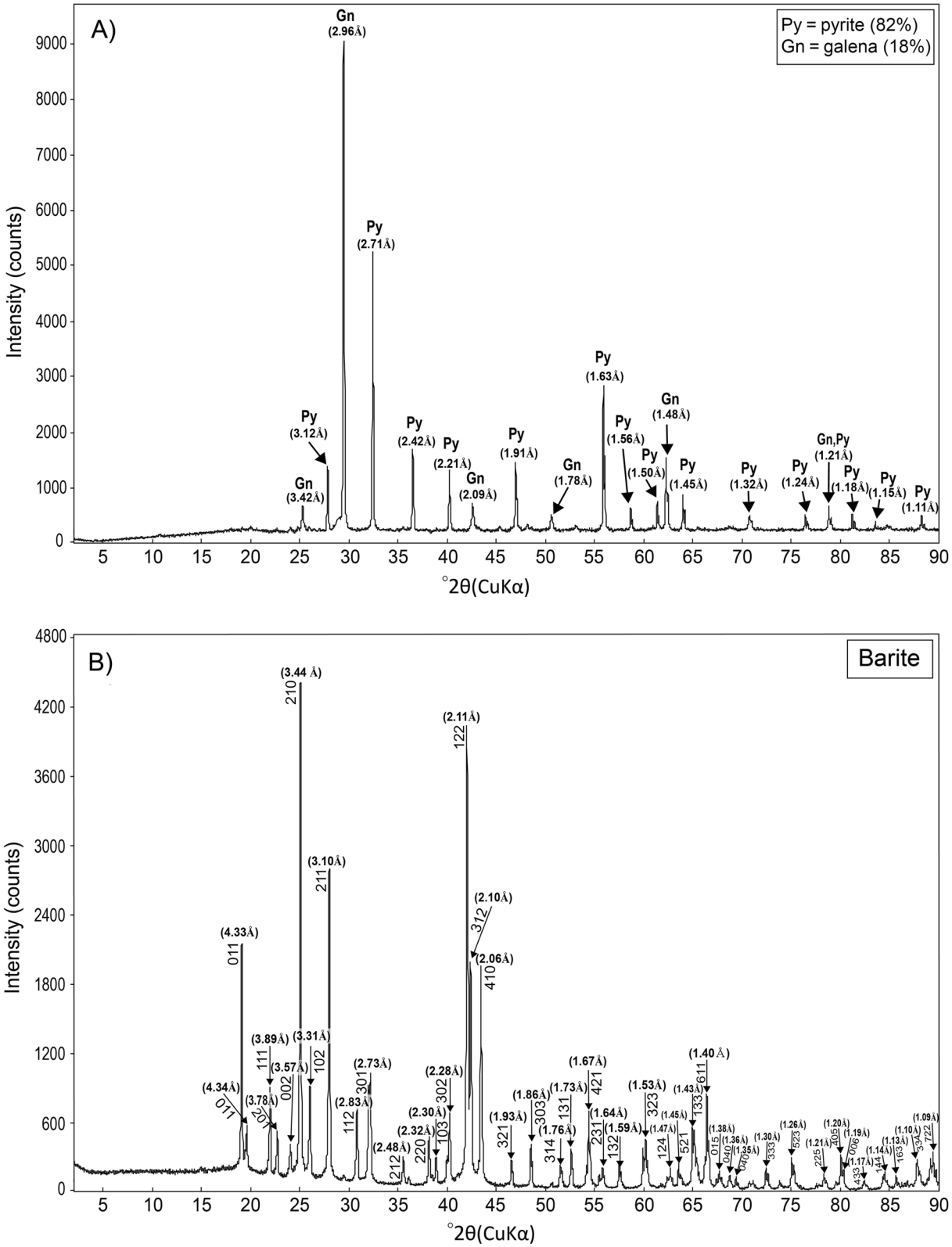

Fig. 2 Mineral identification of **A** a sulfide mixture and **B** barite by XRD analysis

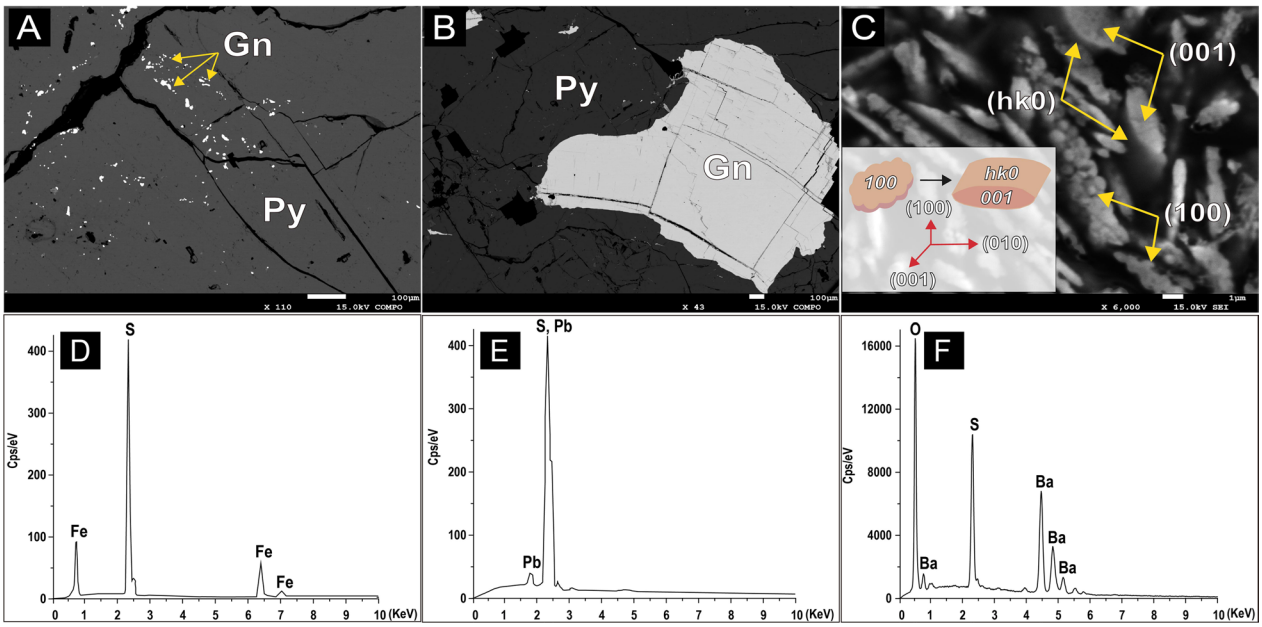

Fig. 3 BSE images of **A** disseminated galena inclusion in pyrite, **B** galena phenocryst in pyrite, and **C** development of barite crystals. EDS spectrums of **D** pyrite, **E** galena, and **F** barite

Table 1 Chemical composition of reactant and product analyzed by energy dispersive spectroscopy (EDS)

Samples	Reactant				Product			
	Pyrite		Galena		Barite			
	Py1	Py2	Gn1	Gn2	Ba1	Ba2	Ba3	Ba4
Oxides (%)								
SO_3	68.95	69.10	24.08	24.28	32.90	33.01	31.90	33.66
FeO	31.05	30.91	1.42	0.63	–	–	–	–
PbO	–	–	74.50	75.09	–	–	–	–
BaO	–	–	–	–	67.10	66.99	68.10	66.34
wt.(%)								
O	48.25	48.47	20.09	20.08	26.72	26.78	26.23	27.10
S	27.61	27.58	9.64	9.72	13.18	13.22	12.77	13.48
Fe	24.14	23.95	1.10	0.49	–	–	–	–
Pb	–	–	69.16	69.71	–	–	–	–
Ba	–	–	–	–	60.10	60.00	61.00	59.42
at. (%)								
O	69.99	70.15	65.75	65.93	66.31	66.34	66.05	66.51
S	19.99	19.92	15.75	15.93	16.31	16.34	16.05	16.51
Fe	10.03	9.93	1.03	0.46	–	–	–	–
Pb	–	–	17.47	17.68	–	–	–	–
Ba	–	–	–	–	17.37	17.31	17.90	16.99
a.p.f.u. based on 24 oxygen atoms								
S	6.85	6.82	5.75	5.80	5.90	5.91	5.83	5.96
Fe	3.44	3.40	0.38	0.17	–	–	–	–
Pb	–	–	6.38	6.43	–	–	–	–
Ba	–	–	–	–	6.29	6.26	6.50	6.13
Cation sum	10.29	10.22	12.50	12.40	12.19	12.18	12.33	12.09

- = below detection limit

Table 2 Sulfur contents and sulfur isotope compositions of samples before and after pretreatments analyzed by elemental analyzer and isotope ratio mass spectrometry (EA/IRMS)

Samples	Material	Chemical formula	S (wt.%)	$\delta^{34}S$ (‰)	SE (±σ)
Reactant					
S1	Pyrite-galena mixture	FeS_2, PbS	46.4	6.98	0.01
S2				6.77	0.07
Product					
A-1	Barite	$BaSO_4$	10.5	6.60	0.08
A-2	Barite	$BaSO_4$	11.4	5.65	0.06
A-3	Barite	$BaSO_4$	11.1	5.53	0.01
A-4	Barite	$BaSO_4$	10.9	6.36	0.05
A-5	Barite	$BaSO_4$	10.8	6.35	0.03
A-6	Barite	$BaSO_4$	11.0	5.51	0.16
A-7	Barite	$BaSO_4$	11.1	5.92	0.15
A-8	Barite	$BaSO_4$	10.1	5.39	0.03
A-9	Barite	$BaSO_4$	10.9	5.56	0.08
A-10	Barite	$BaSO_4$	10.8	6.10	0.11
A-11	Barite	$BaSO_4$	11.0	5.79	0.13

the genesis of ore deposits (Sakai 1968; Bachinski 1969; Li and Liu 2006). According to Bachinski (1969), the bond strength of sulfides is estimated by free energy, lattice energy, and other experimentally obtained empirical methods, and ^{34}S-rich sulfide minerals appear in the following order: pyrite > sphalerite > chalcopyrite > galena. In addition, Ohmoto and Goldhaber (1997) conducted experiments on sulfide minerals (e.g., FeS_2, ZnS, $CuFeS_2$, and PbS) and sulfur ion species (e.g., $SO_{2(gas)}$, $H_2S_{(gas)}$, $S^{2-}{}_{(aq)}$, and $SO_4{}^{2-}{}_{(aq)}$) under equilibrium conditions and systematized the sulfur isotope fractionation that occurs between the two phases according to temperature. When sulfur leached from pyrite (FeS_2) and galena (PbS) forms H_2S, it is fractionated with different sulfur isotope ratios depending on temperature (Ohmoto and Goldhaber 1997). For example, at 200 °C, sulfur isotope ratios increased by + 1.8‰ for pyrite ($FeS_2 \rightarrow H_2S$; Ohmoto and Goldhaber 1997) and decreased by −2.9‰ for galena ($PbS \rightarrow H_2S$; Li and Liu 2006), according to Eqs. 4 and 5, respectively.

$$(FeS_2 \rightarrow H_2S), 1000\ln\alpha = 40 \times \frac{10^6}{T^2(K)} \quad (4)$$

$$(PbS \rightarrow H_2S), 1000\ln\alpha = -0.64 \times \frac{10^6}{T^2(K)} \quad (5)$$

The sulfide used in this study was composed of pyrite and galena, of which the sulfur isotope composition, 6.9‰ on average (n = 2), was approximately 1‰ higher than that of the barite, 5.9‰ on average (5.4–6.6‰, n = 11; Table 2, Fig. 4). When pyrite and galena are converted directly to reduce sulfur gas in a copper reduction tube of the IRMS instrument at temperatures exceeding 1,500 °C, the resulting fractionation effects on sulfur isotopes, as predicted by Eqs. 4 and 5, are less than 0.2‰ and 0.1‰, respectively. Thus, it is unlikely that the isotopic offset would surpass 0.2‰. Our study demonstrates that the fractionation effect of galena, which has a lower sulfur isotope composition than pyrite, is believed to have lowered the isotope value in the process of conversion to H_2S by reacting with the mixed acid at 200 °C. In addition, the sulfur isotope value of the reaction product widely ranged from 5.4 to 6.6‰, this could be attributed to the following reasons: (1) The occurrence form of pyrite and galena, which constitute the sulfides, was irregular; therefore, there was a variation in the leaching rate of sulfur when reacting with the mixed acid, and (2) in the pretreatment process, the mixed solvent boiled before the temperature in the reaction flask reached a temperature of 200 °C, and sulfur was leached early from galena, and at the same time, it fractionated preferentially with a low isotope value in the process of forming H_2S. The magnitude of sulfur isotope fractionation is largely dependent on the sulfide species and temperature conditions. Galena and pyrite, for example, exhibit different degrees of sulfur isotope fractionation when converted to other sulfur species at the same temperature conditions (Ohmoto and Goldhaber 1997; Li and Liu 2006). Kajiwara et al. (1969) studied the fractionation process of sulfur isotopes according to the change in synthesis temperature (150–630 °C) and reaction time (2–180 d), from elemental sulfur to synthetic sulfides, such as pyrite, sphalerite, and galena. Consequently, the sulfur isotope

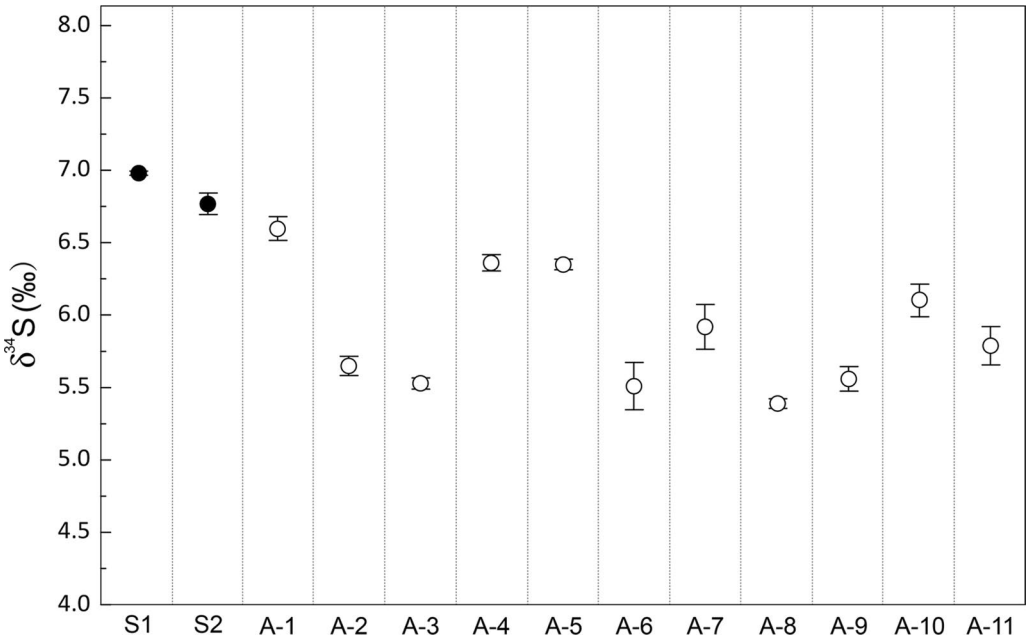

Fig. 4 Variation of sulfur isotope compositions of samples before (solid circle: sulfides) and after (open circle: barite) pretreatments

fractionation factor among the synthesized mineral pairs increased with a decrease in temperature, regardless of the reaction time. Simultaneously, the sulfur isotope values of the synthesized sulfides are known to be heavier in the order of pyrite > sphalerite > galena (Kajiwara et al. 1969). Therefore, the effect of sulfur isotope fractionation between sulfur species by temperature conditions should be considered when performing a series of pretreatment processes for sulfur isotope analysis of a sample composed of a sulfide mixture.

Conclusions

To analyze the sulfur isotope compositions of sulfide minerals from metallic ore deposits, a series of pretreatment processes are required to remove non-analyzed contaminants. In particular, substituting sulfur into the barium sulfate form is an effective method. In this study, during the pretreatment process of sulfides composed of pyrite and galena, H_2S was formed at 200 °C and reacted with an aqueous solution of $Cd(CH_3COO)_2$ to precipitate CdS. Subsequently, H_2O_2 was injected to ionize the sulfate, and barite was recovered by injecting an aqueous solution of $BaCl_2$. The sulfur isotope value of barite (av. 5.9‰), the product, was lower than that of sulfides (av. 6.9‰), the reactant; this seems to be attributed to the fact that sulfur from galena was extracted from the sulfide mixture at an early stage and it fractionated preferentially with a low isotope value during the H_2S-forming process. Therefore, for sulfide mineral composite samples, the effect of sulfur isotope fractionation between sulfur species should be considered when dealing with the isotope values obtained from the pretreatment process.

Abbreviations

CDT	Canyon Diablo Troilite
XRD	X-ray diffraction
FE-SEM	Field emission scanning electron microscopy
EDS	Energy-dispersive X-ray spectroscopy
EA	Elemental analyzer
IRMS	Isotope ratio mass spectrometer

Acknowledgements

We appreciate the Instrumental Analysis Center of Gyeongsang National University for technical support. The manuscript benefited significantly from critical reviews and valuable comments by two anonymous reviewers and associate editor.

Author contributions

JJ was involved in conceptualization, methodology, visualization, and writing. DS contributed to conceptualization, methodology, and reviewing. TY and HC helped in conceptualization and methodology. All authors read and approved the final manuscript.

Funding

This research was supported by the National University Development Project by the Ministry of Education of Kora in 2022 and by the National Research Foundation of Korea (NRF) grant funded by the Ministry of Education (MOE) (No. 2020R1I1A1A01058214) and the Ministry of Science and ICT (MSIT) (Nos. 2019R1A2C1085334, 2021M2E1A1099413, 2022R1A2C1008260).

Availability of data and materials

All data generated or analyzed during this study are included in this published article.

Declarations

Competing interests

The authors declare that they have no competing interests.

Received: 11 January 2023 Accepted: 4 May 2023
Published online: 09 May 2023

References

Abraitis PK, Pattrick RAD, Vaughan DJ. Variations in the compositional, textural and electrical properties of natural pyrite: a review. Int J Miner Process. 2004;74:41–59. https://doi.org/10.1016/j.minpro.2003.09.002.

Arnold GL, Brunner B, Müller IA, Røy H. Modern applications for a total sulfur reduction distillation method-what's old is new again. Geochem Trans. 2014;15:4. https://doi.org/10.1186/1467-4866-15-4.

Ault WU, Kulp JL. Isotopic geochemistry of sulphur. Geochim Cosmochim Acta. 1959;16:201–35. https://doi.org/10.1016/0016-7037(59)90112-7.

Bachinski DJ. Bond strength and sulfur isotopic fractionation in coexisting sulfides. Econ Geol. 1969;64:56–65. https://doi.org/10.2113/gsecongeo.64.8.934.

Basu A, Schreiber ME. Arsenic release from arsenopyrite weathering: Insights from sequential extraction and microscopic studies. J Hazard Mater. 2013;262:896–904. https://doi.org/10.1016/j.jhazmat.2012.12.027.

Beaudoin G, Taylor BE, Rumble D, Thiemens M. Variations in the sulfur isotope composition of troilite from the Cañon Diablo iron meteorite. Geochim Cosmochim Acta. 1994;58:4253–5. https://doi.org/10.1016/0016-7037(94)90277-1.

Grassineau NV. High-precision EA-IRMS analysis of S and C isotopes in geological materials. Appl Geochem. 2006;21:756–65. https://doi.org/10.1016/j.apgeochem.2006.02.015.

Grootenboer J, Schwarcz HP. Experimentally determined sulfur isotope fractionations between sulfide minerals. Earth Planet Sci Lett. 1969;7:162–6. https://doi.org/10.1016/0012-821X(69)90031-4.

Halas S, Szaran J. Improved thermal decomposition of sulfates to SO_2 and mass spectrometric determination of $\delta^{34}S$ of IAEA SO-5, IAEA SO-6 and NBS-127 sulfate standards. Rapid Commun Mass Spectrom. 2001;15:1618–20. https://doi.org/10.1002/rcm.416.

Hutchison W, Finch AA, Boyce AJ. The sulfur isotope evolution of magmatic-hydrothermal fluids: insights into ore-forming processes. Geochim Cosmochim Acta. 2020;288:176–98. https://doi.org/10.1016/j.gca.2020.07.042.

Kajiwara Y, Krouse HR, Sasaki A. Experimental study of sulfur isotope fractionation between coexistent sulfide minerals. Earth Planet Sci Lett. 1969;7:271–7. https://doi.org/10.1016/0012-821X(69)90064-8.

Kawasumi S, Chiba H. Redox state of seafloor hydrothermal fluids and its effect on sulfide mineralization. Chem Geol. 2017;451:25–37. https://doi.org/10.1016/j.chemgeo.2017.01.001.

Li Y, Liu J. Calculation of sulfur isotope fractionation in sulfides. Geochim Cosmochim Acta. 2006;70:1789–95. https://doi.org/10.1016/j.gca.2005.12.015.

Liu S, Li Y, Liu J, Shi Y. First-principles study of sulfur isotope fractionation in pyrite-type disulfides. Am Mineral. 2015;100:203–8. https://doi.org/10.2138/am-2015-5003.

Macnamara J, Thode HG. Comparison of the isotopic constitution of terrestrial and meteroritic sulfur. Phys Rev. 1950;78:307–8. https://doi.org/10.1103/PhysRev.78.307.

Monaghan JM, Scrimgeour CM, Stein WM, Zhao FJ, Evans EJ. Sulphur accumulation and redistribution in wheat (*Triticum aestivum*): a study using stable sulphur isotope ratios as a tracer system. Plant Cell Environ. 1999;22:831–9. https://doi.org/10.1046/j.1365-3040.1999.00445.x.

Ohmoto H, Goldhaber MB. Sulfur and carbon isotopes. In: Barnes HL, editor. Geochemistry of hydrothermal ore deposits. 3rd ed. New York: John Wiley; 1997. p. 517–611.

Pokrovski GS, Kara S, Roux J. Stability and solubility of arsenopyrite, FeAsS, in crustal fluids. Geochim Cosmochim Acta. 2002;66:2361–78. https://doi.org/10.1016/S0016-7037(02)00836-0.

Ren Y, Wohlgemuth-Ueberwasser CC, Huang F, Shi X, Li B, Oelze M, Schreiber A, Wirth R. Distribution of trace elements in sulfides from Deyin hydrothermal field, Mid-Atlantic Ridge—Implications for its mineralizing processes. Ore Geol Rev. 2021;128:103911. https://doi.org/10.1016/j.oregeorev.2020.103911.

Román N, Reich M, Leisen M, Morata D, Barra F, Deditius AP. Geochemical and micro-textural fingerprints of boiling in pyrite. Geochim Cosmochim Acta. 2019;246:60–85. https://doi.org/10.1016/j.gca.2018.11.034.

Sakai H. Isotopic properties of sulfur compounds in hydrothermal processes. Geochem J. 1968;2:29–49. https://doi.org/10.2343/geochemj.2.29.

Salomons W. Isotope fractionation between galena and pyrite and between pyrite and elemental sulfur. Earth Planet Sci Lett. 1971;11:236–8. https://doi.org/10.1016/0012-821X(71)90169-5.

Sasaki A, Arikawa Y, Folinsbee RE. Kiba reagent method of sulfur extraction applied to isotopic work. Bull Geol Surv Jpn. 1979;30:241–5.

Spangenberg JE, Saintilan NJ, Palinka SS. Safe, accurate, and precise sulfur isotope analyses of arsenides, sulfarsenides, and arsenic and mercury sulfides by conversion to barium sulfate before EA/IRMS. Anal Bioanal Chem. 2022;414:2163–79. https://doi.org/10.1007/s00216-021-03854-y.

Studley SA, Ripley EM, Elswick ER, Dorais MJ, Fong J, Finkelstein D, Pratt LM. Analysis of sulfides in whole rock matrices by elemental analyzer–continuous flow isotope ratio mass spectrometry. Chem Geol. 2002;192:141–8. https://doi.org/10.1016/S0009-2541(02)00162-6.

Thode HG, Monster J, Dunford HB. Sulphur isotope geochemistry. Geochim Cosmochim Acta. 1961;25:159–74. https://doi.org/10.1016/0016-7037(61)90074-6.

Toshiyasu K, Ikuko A, Nobuyuki S. Rapid determination of inorganic sulfur in various forms, particularly in sulfide ores, by the tin (II)-strong phosphoric acid reduction method. Bull Geol Surv Jpn. 1957;30:972–5. https://doi.org/10.1246/bcsj.30.972.

Yanagisawa F, Sakai H. Thermal decomposition of barium sulfate-vanadium pentoxide-silica glass mixtures for preparation of sulfur dioxide in sulfur isotope ratio measurements: Anal. Chem. 1983;55:985–7. https://doi.org/10.1021/ac00257a046.

Zhang J. Equilibrium sulfur isotope fractionations of several important sulfides. Geochem J. 2021;55:135–47. https://doi.org/10.2343/geochemj.2.0623.

Publisher's Note